IDŐJÁRÁS

Quarterly Journal of the Hungarian Meteorological Service
Vol. 119, No. 4, October – December, 2015, pp. 515–535

Continentality in Europe according to various resolution regional climate models with A1B scenario in the 21st century

Beáta Szabó-Takács[1]*, **Aleš Farda**[1,3], **Pavel Zahradníček**[1,2], and **Petr Štěpánek**[1,2]

[1] *Global Change Research Centre AS CR, v.v.i.*
Bělidla 986/4a, 60300 Brno, Czech Republic

[2] *Czech Hydrometeorological Institute, branch Brno,*
Kroftova 43, 616 00 Brno, Czech Republic

[3] *Czech Hydrometeorological Institute,*
Na Šabatce 17, 143006 Prague, Czech Republic

** Corresponding authors E-mail: szabo.b@czechglobe.cz*

(Manuscript received in final form January 8, 2015)

Abstract— The purpose of our research is to simulate the influence of the thermal properties of land surface on the Central European climate in the 21st century. The simulation is carried out with calculation of Gorczynsky and Conrad continentality indexes, respectively, as a function of annual temperature range. Seven different ENSEMBLES models (ARPÈGE, CNRM, DMI, ITCP, KNMI, MPI, and SMHI) with various resolutions perform the space difference of continentality between seven European regions with IPCC A1B emission scenario for two time slices: 2021–2050 and 2071–2100. Beside these models, ALADIN-Climate/CZ simulation is implemented in finer resolution and smaller CECILIA domain taking into consideration only the central European area. The bias correction of models is implemented using the European Climate Assessment and Dataset (ECA&D). The largest influence to the spread among the simulation results is due to the chosen global climate models (GCMs). The resolution differences do not play dominant role in the variance of the results against the domain size. There are not significant differences between the Gorczynsky and Conrad index values. The largest change in the climate type tendency is simulated in the Scandinavian region by the Gorczynsky approach. In central Europe, the climate becomes continental only according to CNRM result which correlates with its underestimation of precipitation and overestimation of temperature. The simulated continentality indexes and the predicted changes are presented here.

Key-words: continentality, Gorczynsky index, Conrad index, ENSEMBLES, climate change, E-OBS

1. Introduction

Continentality is a basic indicator of climate change. In the climate of central Europe, oceanic and continental climate effects are combined. The continental climate areas have great annual temperature range and moderate precipitation (*McBoyle* and *Steiner,* 1972), whilst the oceanic climate is more balanced. The reason of this basic difference comes from the different thermal properties of ocean and land surface. The oceans have larger heat capacity, whilst the inland has larger heat conduction, which depends on surface properties (*Nikiforova et al*., 2013). The combination of heat capacity and thermal conductivity determines three important physical properties underlying climate: (i) the proportion of heat shared by the interface substances; (ii) the depth (soil, water) or height (atmosphere) to which heat flows or transported; (iii) the range of temperatures over diurnal and annual cycles (*Dirscoll* and *Yee Fong,* 1992). This phenomenon has an effect on several climatic elements like distribution of cloudiness, precipitation, etc., which impact the temperature anomaly. Different approaches are used to quantify continentality (*Gorczynsky,* 1922; *Johansson,* 1926; *Conrad* and *Pollak,* 1950; *Currey,* 1974; *Holmlund* and *Schneider,* 1997; *Sládek,* 2005; *Mikolaskova,* 2009).

The purpose of our work is to investigate the formation of the spatial differences of continentality in Central Europe using ENSEMBLES based on A1B SRES scenario in the 21th century. The A1B estimates the future world in perspective of technical change in energy system with the assumption that similar improvement rates apply to all energy supply and end use technologies (*Nakićenovíc,* 2000*, Solomon,* 2007).

The EU 6th Framework Programme project ENSEMBLES applies a probabilistic approach to climate changes at a regional scale (*Hewit* and *Griggs,* 2004) with downscaling global circulation models (GCM) to higher resolution regional climate models (*van der Linden* and *Mitchell,* 2009).

The sources of uncertainties in the ENSEMBLES predictions are the chosen GCM, RCM, downscaling technique, and natural variability. The choice of GCM significantly determines the initial and boundary conditions of RCMs. The source of differences in RCMs comes from the difference of the applied physical parameterizations to represent sub-grid effects. There are two basic downscaling techniques: dynamical and statistical. The dynamical downscaling is not able to improve the simulation skills of large-scale fields over those simulated by the GCM (*Dosio* and *Paruolo,* 2011), while the statistical relationship is developed for present day climate by statistical downscaling is assumed to be valid for future climate under different forcing condition (*Wilby et al.,* 1998). The natural variability, such as seasonal cycle of insolation, non-linear interplay of feedbacks, and random fluctuations in physical or chemical factors also has an effect on the uncertainties. *Déqué et al*. (2012) found that the natural variability produces significantly larger mean interannual spread in a given model than running an ensemble of the same size without considering perturbing the parameters. According to *Kjellström et al.* (2011), the lower natural variability in ECHAM5 and smaller large-scale circulation changes in HadCM3 (ECHAM5-r2 and HadCM3-low) show larger warming in much of Europe than the larger one (ECHAM5-r3 and HadCM3-high).

2. Data and method

The calculations were implemented in the variable resolution ARPÈGE 4. atmospheric global climate model (AGCM), and in six different 25 km resolution regional climate models (RCMs) for the European area using Gorzynsky and Conrad indexes, respectively. The resolution of ARPÈGE is 50 km over Central Europe and decreases to 300 km at the antipodes. The ENSEMBLES models chosen for our study are shown in *Table 1*. They are representative selection of models with respect to GCMs/RCMs combination. The temperature anomaly and continentality were predicted for 2021–2050 and 2071–2100.

Table 1. The institute, reference, GCM, RCM, and resolution of chosen ENSEMBLES simulations

	INSTITUTE/ REFERENCE	**GCM**	**RCM**	**RESOULTION**
1	ARPÈGE *Gibelin* and *Déqué*, (2003)	ARPÈGE	-	50 km
2	CNRM/ *Déqué* (2007)	ARPÈGE	ALADIN	25 km
3	DMI/ *Christensen et al*. (1996)	ARPÈGE	HIRHAM	25 km
4	KNMI/ *Lenderink et al*. (2003)	ECHAM5-r3	RACMO	25 km
5	SMHI/ *Kjellström et al*. (2005)	ECHAM5-r3	RCA	25 km
6	MPI/ *Jacob* (2001)	ECHAM5-r3	REMO	25 km
7	ICTP/ *Giorgi et al*. (2004)	ECHAM5-r3	RegCM	25 km
8	CHMI/ *Farda et al*. (2007)	ARPÈGE	ALADIN/CZ	10 km

Since the models contain bias, it is necessary to correct their outputs. An important point in the correction is the availability of suitable reference data, e.g., observations or re-analyses. On the European level, the biggest database of daily meteorological station observations is the European Climate Assessment and Dataset (ECA&D). The ECA&D project (*Klein Tank et al.,* 2002) was initiated by the European Climate Support Network of EUMETNET in 2002, and it was coordinated by the Royal Netherlands Meteorological Institute

(KNMI). ECA&D daily database contains more than 31k quality controlled series of 12 climate variables at more than 7000 meteorological stations in 62 countries, from which about half of them are public (*Fig. 1*). Using the ECA&D blended daily station data, the E-OBS daily high-resolution gridded observational dataset was produced. The E-OBS (*Haylock et. al.,* 2008) is currently perhaps the best pan-European gridded dataset with the spatial resolution of 0.25º in longitude and latitude (or 0.22º on the rotated pole grid typical for many RCMs) covering the period from 1950.

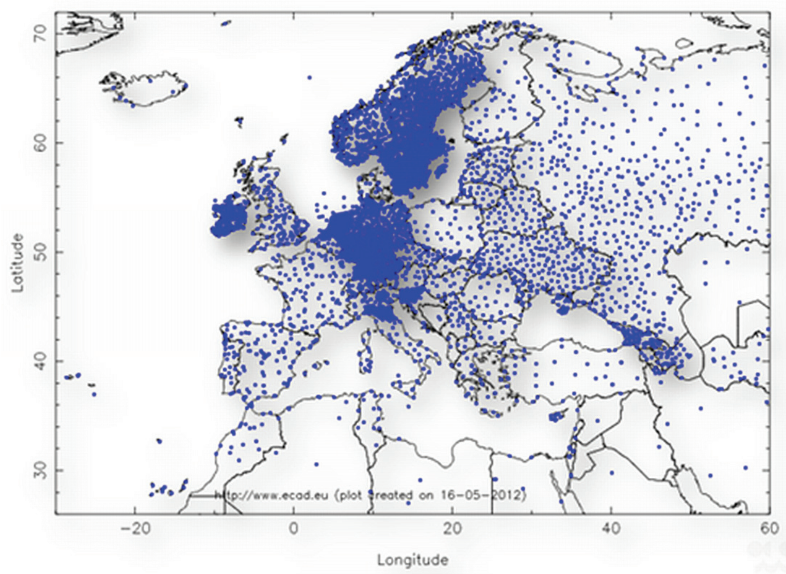

Fig. 1. Meteorological stations of ECA&D database.

The RCMs were corrected on the monthly scale. In the first step for each RCM grid point, the nearest E-OBS grid points were found. The differences of control run of RCM models and E-OBS database (applying reference period 1961–2000) were calculated for each month individually. Found differences were used for correcting the RCM outputs. It has been calculated for more than 14,000 grid points.

Considering the Central European area (Czech Republic (CR), Slovakia (SK), North-East Austria (AT)), the calculations were carried out with the 10 km resolution ALADIN/CZ RCM (*Fig. 2*). The regional climate model ALADIN - Climate/CZ is an adaptation of ALADIN numerical weather prediction model, version CY28T3. Within the EU FP6 project CECILIA, it was coupled with the GCM ARPEGE to provide a projection of future climate in two time slices, 2021–2050 and 2071–2100, according to the IPCC A1B emission scenario. Its description can be found, e.g., in *Farda et al.* (2007) or *Farda et al.* (2010). Before the analysis of the future climate, the model data were corrected, in daily step, according to validation results carried out for the period 1961-2000. For this purpose (comparison with "truth"), the so-called technical series were recalculated from station data in the positions of grid points of the model (ALADIN-Climate/CZ grid at 10 km horizontal resolution, for the details about the method see, e.g., *Štěpánek et al.,* 2011a). All input station observations were quality controlled, homogenized in daily scale, and gaps in data were filled (for more information about the preprocessing of station data please refer to *Štěpánek et al.,* 2011b, 2013). According to the relationship between the RCM outputs and the recalculated station data (technical series for the grid points), outputs of A1B scenario integrations of the future climate were corrected applying an approach of *Déqué et al.* (2007) that is based on a variable correction using individual percentiles. The model outputs are fully compatible with the station (measured) data. As mentioned above, these data were processed at daily scale, from which final monthly values were then calculated. All data processing was performed by ProClimDB database software for processing of climatology datasets (free download is possible from www.climahom.eu).

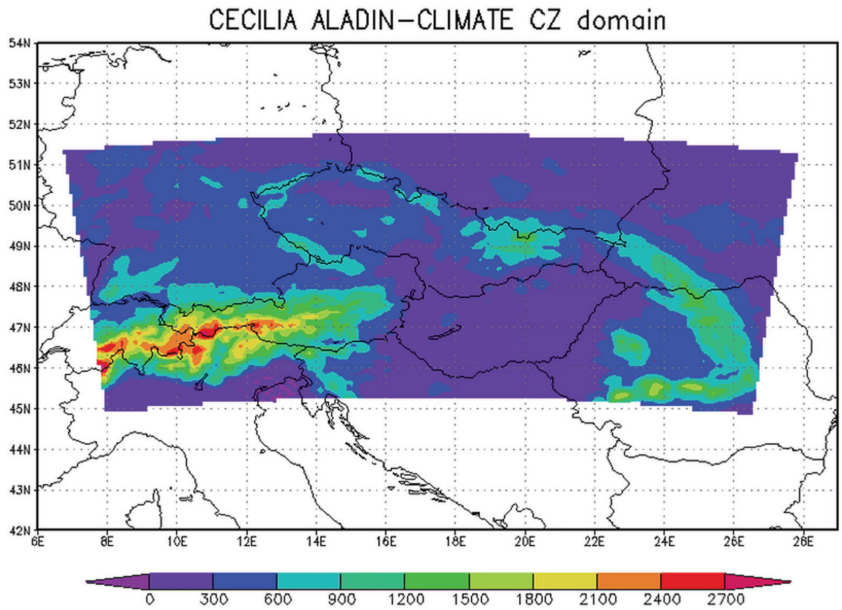

Fig. 2. Integration area with orography and used grid points details of model ALADIN-Climate/CZ as used in EC FP6 CECILIA project.

Owing to the higher density station network used for the correction, this dataset is expected to be subject of smaller interpolation error than E-OBS (*Hofstra et al.,* 2010).

The continentality index is calculated as a function of annual temperature anomaly divided by the sine of latitude to compensate for seasonal differences in radiation. The Gorzynsky index is most commonly used in Europe. It is computed by the equation:

$$k = \frac{1.7(A - 12\sin\theta)}{\sin\theta} = \frac{1.7A}{\sin\theta} - 20.4\,, \tag{1}$$

where A is the mean annual anomaly of temperature in °C, and θ is the latitude in degree. According to *Gorczynsky* (1922), the expression of A=12sinθ corresponds well with observation over the ocean. The 1.7 constant is calculated from the assumption that Verchojansk, in eastern Siberia, is representative of 100% continentality (*Mikolaskova,* 2009). Based on the equation, the continentality can be divided into three categories: transitional maritime (k=0 to 33%), continental (k=33 to 66%), and extreme continental (k=67 to 100%) *Gorczynsky* (1922).

Conrad and *Pollak* (1950) found that the Gorczynsky approach gives negative values, which does not have physical meaning in some particular locations (e.g., Thorshvan at Faeroe Islands), hence they modified the equation with taking into account boundary conditions. The Conrad continentality index can be calculated by the equation:

$$k = \frac{1.7A}{\sin(\theta + 10)} - 14\,. \tag{2}$$

If the index value is 0, the climate is no longer influenced by continental surface, and if the value is 100, the climate is no longer influenced by maritime air masses (*Mikolaskova,* 2009). This index reaches better results in lower latitudes (e.g., 0), but its results are invalid in latitudes higher than 80.

The Pan-European domain originally designed for the ENSEMBLES project (*van der Linden* and *Mitchell,* 2009) is divided into seven regions for investigating the spatial differences of ENSEMBLES predicted annual temperature anomaly and continentality. The chosen regions are Southern Europe (1), Western Europe (2), Great Britain (3), Scandinavia (4), Central Europe (5), South-Eastern Europe (6), and Eastern Europe (7) represented in *Fig. 3*.

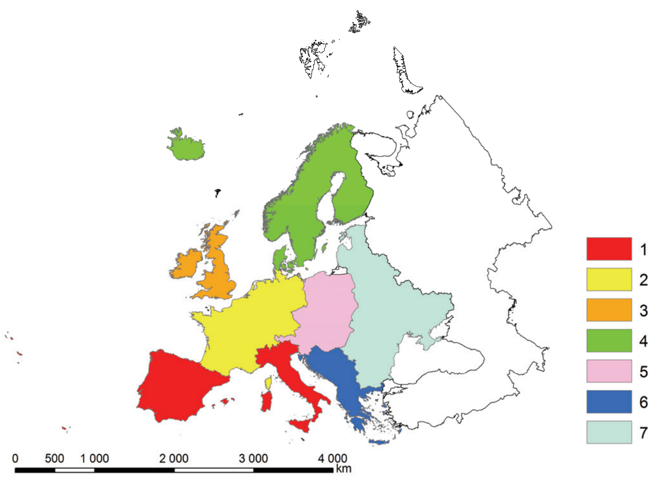

Fig. 3. Regions of ENSEMBLES domain: 1. South Europe, 2. Western Europe, 3. Great Britain, 4. Scandinavia, 5. Central Europe, 6. South-East Europe, and 7. East-Europe.

3. Results

3.1. Temperature anomaly

Table 2 shows the predicted mean annual temperature anomaly in the different regions in the 2021–2050 and 2071–2100 periods. The mean values denote that the temperature range increases eastward and toward the center of South Europe in both time periods. Increasing the distance from the Atlantic Ocean increases the temperature anomaly toward the east direction. The larger anomaly in South Europe can be explained with the topography, which modifies the intensity and depth of penetration of maritime influences. This block of wet maritime airmass is combined with rise of aridity which increases the temperature anomaly (*Dirscoll* and *Yee Fong*, 1992).

Table 2. Predicted mean annual temperature amplitudes T_{mean} in 2021–2050 (top) and 2071–2100 (bottom) for the defined regions: South Europe (1), Western Europe (2), Great Britain (3), Scandinavia (4), Central Europe (5), South-East Europe (6), East-Europe (7)

	Temperature amplitude in 2021–2050						
Region	**ARPÈGE** T_{mean}	**CNRM** T_{mean}	**DMI** T_{mean}	**ICTP** T_{mean}	**KNMI** T_{mean}	**MPI** T_{mean}	**SMHCI** T_{mean}
1	18.8	18.8	18.3	19.0	19.0	19.1	19.4
2	18.3	18.5	18.0	17.9	18.0	18.0	17.8
3	13.0	13.2	12.7	13.0	12.9	12.8	12.6
4	22.6	22.9	22.7	23.1	23.1	22.6	22.7
5	22.0	21.9	21.8	21.3	21.4	21.2	21.0
6	22.7	22.6	21.5	21.4	21.4	21.4	21.3
7	26.4	26.2	25.5	24.7	24.9	24.5	24.4
	Temperature amplitude in 2071–2100						
Region	**ARPÈGE** T_{mean}	**CNRM** T_{mean}	**DMI** T_{mean}	**ICTP** T_{mean}	**KNMI** T_{mean}	**MPI** T_{mean}	**SMHCI** T_{mean}
1	20.4	20.5	20.0	20.7	20.8	21.0	21.1
2	20.0	20.9	19.4	18.3	18.7	18.1	18.1
3	13.1	13.8	13.0	12.9	12.9	12.6	12.4
4	21.2	21.7	21.2	21.5	21.5	21.2	20.5
5	23.3	24.6	22.6	21.0	21.6	20.6	20.7
6	24.7	24.9	23.1	22.2	22.5	22.4	22.5
7	27.4	27.7	25.8	24.7	25.1	24.1	24.2

In 2021–2050, the spread among the predicted mean annual temperature anomalies are smaller than 0.3 in the Western Europe, Great-Britain, and Scandinavia regions (*Table 3a*). In the other regions, differences appear between ARPÈGE and ECHAM5-r3 driven RCMs results, respectively. The temperature range values are higher for RCMs forced by ARPÈGE except in South Europe. The ECHAM5 driver is coupled ocean-atmosphere GCM, while ARPÈGE is forced by the SST and sea-ice conditions of ERA40 (*Déqué* personal discussion) with added delta monthly anomaly from HadCM3 GCM (*Déqué,* 2007). The sea-ice extension is overestimated by HadCM3_ref, while it is underestimated by ECHAM5. Large-scale circulation in ECHAM5 is too zonal which transports the cool and moist air from the North Atlantic in summer (*Kjellström et al.,* 2011), and warm air is advected from the North Atlantic into the Baltic Sea region in winter combined with reduction of sea-ice albedo (*Meier et al.,* 2011). This too strong influence of the Atlantic Ocean on the surface temperature also contributes to the climate of the Central European regions, where it reduces the continental influences (*Plavcová* and *Kyselý*, 2011). The variability of the models is the largest in Scandinavia, which can also contribute to the SST and sea-ice condition caused natural variability.

The predicted change values are calculated by differences between the model predicted future (T_M) and E-OBS measured present (T_E) mean temperature anomalies. These values are negative in both RCMs in Scandinavia and in the ECHAM5 driven RCMs in Central and East Europe too, respectively. These negative values mean that the climate will be more balanced in the future than in the present. ARPÈGE has the largest positive differences in South-East Europe due to the increasing drought resulted from underestimating the precipitation in summer (*Gibelin* and *Déqué,* 2003; *Déqué,* 2007).

Compared with the 2021–2050 term, the mean annual temperature spread among the models increases in each regions in the 2071–2100 time period. Its largest value is 1.5 in Central Europe and the smallest is in Scandinavia region (*Table 3b*). In Central Europe, the mean annual temperature range increases in ARPÈGE driven RCMs and diminishes in ECHAM5 forced ones except KNMI compared with the 2021–2050 period. Moreover, the boundaries of the anomaly become slantwise to south-west north-east direction (not shown).

The mean annual temperature anomalies are also larger in RCMs forced with ARPÈGE except in South Europe. CNRM has the largest mean annual temperature anomalies and the highest predicted change in Central, South-East, and East Europe. SMHCI results the smallest mean annual temperature anomaly except in South Europe and Scandinavia. The variability of the models increases in each region in time with exception of Scandinavia area (not shown). Its value is higher in both time period due to the higher natural variability of the ECHAM5 forced RCMs (denoted by -r3). Because SSTs and sea-ice conditions are significant 'red noise' components (*Hasselmann,* 1976*; Rowell* and *Zwiers,* 1999), the reduction of model variability in time refers to the fact that the signal (global warming) to noise (natural variability) is greater than in the former period.

In the most regions, the predicted change values increase with time (not shown). CNRM has the largest change values except in the Scandinavia area.

Table 3a. The spread of the simulated temperature amplitude of the models in 2021–2050 for the regions defined in *Table 2*

Spread of simulated temperature amplitude 2025-2050							
	1	**2**	**3**	**4**	**5**	**6**	**7**
ARPÈGE	18.8	18.3	13	22.6	22	22.7	26.4
CNRM	18.8	18.5	13.2	22.9	21.9	22.6	26.2
DMI	18.3	18	12.7	22.7	21.8	21.5	25.5
ICTP	19	17.9	13	23.1	21.3	21.4	24.7
KNMI	19	18	12.9	23.1	21.4	21.4	24.9
MPI	19.1	18	12.8	22.6	21.2	21.4	24.5
SMHCI	19.4	17.8	12.6	22.7	21	21.3	24.4
mean	**18.91**	**18.07**	**12.88**	**22.81**	**21.51**	**21.75**	**25.22**
spread	**0.33**	**0.24**	**0.20**	**0.21**	**0.38**	**0.61**	**0.81**

Table 3b. The spread of the simulated temperature amplitude of the models in 2071–2100 for the regions defined in *Table 2*

Spread of simulated temperature amplitude 2070–2100							
	1	**2**	**3**	**4**	**5**	**6**	**7**
ARPÈGE	20.4	20	13.1	21.2	23.3	24.7	27.4
CNRM	20.5	20.9	13.8	21.7	24.6	24.9	27.7
DMI	20	19.4	13	21.2	22.6	23.1	25.8
ICTP	20.7	18.3	12.9	21.5	21	22.2	24.7
KNMI	20.8	18.7	12.9	21.5	21.6	22.5	25.1
MPI	21	18.1	12.6	21.2	20.6	22.4	24.1
SMHCI	21.1	18.1	12.4	20.5	20.7	22.5	24.2
mean	**20.64**	**19.07**	**12.95**	**21.25**	**22.05**	**23.18**	**25.57**
spread	**0.37**	**1.07**	**0.44**	**0.38**	**1.50**	**1.13**	**1.46**

3.2. Gorczynsky index

The predicted mean Gorczynsky continentality indexes (Eq. (1)) in the 2021–2051 and 2071–2100 time slices are demonstrated in *Table 4*. According to the Gorczynsky index, the boundary of transitional maritime and continental climate is 33%. This boundary is near meridional in East Europe and against with *Mikolaskova,* 2009 results. Its direction is eastward in South-East and South Europe, respectively, in the 2021–2050 time slice (*Fig. 4*). The differences between the ARPÈGE and ECHAM5 driven model predicted indexes are analogous with the temperature amplitude ones.

In the 2021–2050 period, the climate is continental in South East and East Europe according to each model. The spread among the model results is smaller than 0.5 in Great Britain and Scandinavia, while it is greater than 1.0 in South East and East Europe (*Table 5a*).

The predicted change values are also negative in Scandinavia in case of each model and in Central and East Europe, respectively, in case of ECHAM5 forced RCMs (*Fig. 4*). The SMCHI has negative difference value in each region except for South- and South-East Europe, respectively, which relates with its smallest temperature anomaly values.

Correlating with temperature anomaly change, the Gorczynsky index depicts a sharp changing in the 2071–2100 period, where the continental climate slopes toward the north-east south-west direction. The continental climate recedes toward the southern direction in Scandinavia area, but increases in South and South-East Europe in both model cases. With exception of the Scandinavia area, index value increases in RCMs which are forced with ARPÈGE compared to the former period. In case of ECHAM5 driven RCMs, it decreases in more regions. The continentality rises in Central Europe only according to KNMI among ECHAM5 driven RCMs. In Central Europe, the continental climate predominates according to CNRM only where the index mean value is 34.5. CNRM has the largest mean annual temperature anomaly and the largest predicted change value in Central Europe in this period. *Christensen et al,* (2008) found that CNRM ALADIN has the largest positive temperature and negative precipitation biases from E-OBS observed data in Central European region compared with DMI, ICTP, KNMI, MPI, and SMHCI, when the RCMs were forced with ERA40. The spread among the model results is also the smallest in Scandinavia and Great Britain and the largest in South East and East Europe (*Table 5b*). The predicted change tendency is also analogous with the change of temperature range.

Table 4. Space differences of the predicted mean Gorczynsky index G_{mean} in 2021–2050 (top) and 2071–2100 (bottom) for the regions defined in *Table 2*

	Gorczynsky index in 2021–2050						
Region	**ARPÈGE** G_{mean}	**CNRM** G_{mean}	**DMI** G_{mean}	**ICTP** G_{mean}	**KNMI** G_{mean}	**MPI** G_{mean}	**SMHCI** G_{mean}
1	28.4	28.5	27.1	29.1	29.1	29.2	29.9
2	21.5	21.8	20.8	20.6	20.6	20.6	20.2
3	7.1	7.5	6.6	7.0	7.0	6.7	6.4
4	22.8	23.2	22.9	23.6	23.7	22.8	22.8
5	28.7	28.4	28.1	27.2	27.2	26.9	26.3
6	37.2	36.7	34.0	33.8	33.8	33.7	33.6
7	39.2	38.8	37.2	35.3	35.7	34.9	34.6
	Gorczynsky index in 2071–2100						
Region	**ARPÈGE** G_{mean}	**CNRM** G_{mean}	**DMI** G_{mean}	**ICTP** G_{mean}	**KNMI** G_{mean}	**MPI** G_{mean}	**SMHCI** G_{mean}
1	32.6	32.7	31.6	33.3	33.8	34.1	34.6
2	25.5	27.3	24.0	21.3	22.3	21.1	21.0
3	7.5	8.9	7.1	6.8	6.8	6.3	5.9
4	20.1	21.0	20.0	20.4	20.6	20.0	18.7
5	31.5	34.5	30.1	26.2	27.8	25.5	25.7
6	42.0	42.5	38.1	35.8	36.5	36.3	36.7
7	41.6	42.2	38.0	35.3	36.3	34.0	34.3

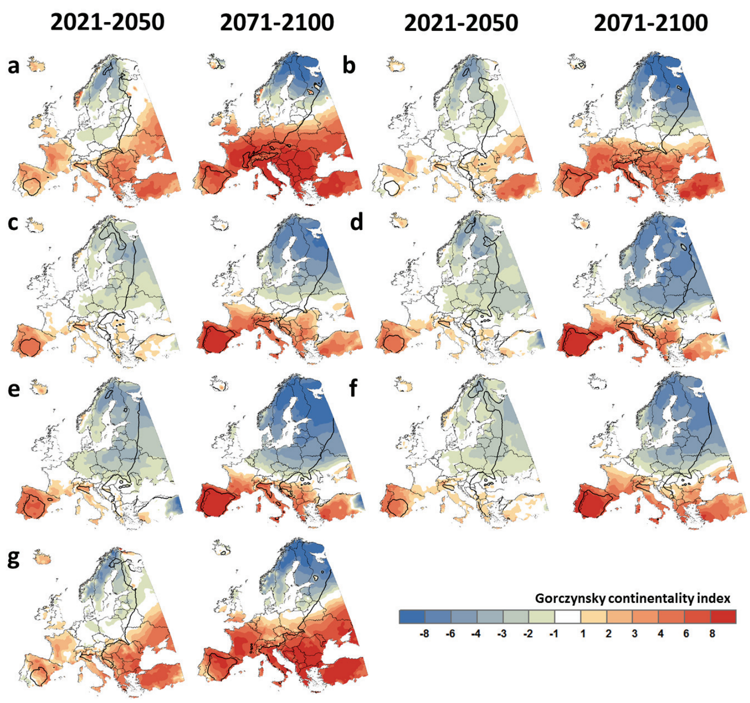

Fig. 4. Predicted changes of Gorczynsky indexes (a) CNRM, (b) DMI, (c) KNMI, (d) MPI, (e) SMHIRCA, (f) ICTP, and (g) ARPÈGE.

Table 5a. The spread of the simulated Gorczynsky index of the models in 2021–2050 for the regions defined in *Table 2*

Spread of simulated Gorczynsky index 2025-2050							
	1	**2**	**3**	**4**	**5**	**6**	**7**
ARPÈGE	28.4	21.5	7.1	22.8	28.7	37.2	39.2
CNRM	28.5	21.8	7.5	23.2	28.4	36.7	38.8
DMI	27.1	20.8	6.6	22.9	28.1	34	37.2
ICTP	29.1	20.6	7	23.6	27.2	33.8	35.3
KNMI	29.1	20.6	7	23.7	27.2	33.8	35.7
MPI	29.2	20.6	6.7	22.8	26.9	33.7	34.9
SMHCI	29.9	20.2	6.4	22.8	26.3	33.6	34.6
mean	**28.75**	**20.87**	**6.9**	**23.11**	**27.54**	**34.68**	**36.52**
spread	**0.88**	**0.56**	**0.36**	**0.39**	**0.87**	**1.55**	**1.88**

Table 5b. The spread of the simulated Gorczynsky index of the models in 2071–2100 for the regions defined in *Table 2*

Spread of simulated Gorczynsky index 2070-2100							
	1	**2**	**3**	**4**	**5**	**6**	**7**
ARPÈGE	32.6	25.5	7.5	20.1	31.5	42	41.6
CNRM	32.7	27.3	8.9	21	34.5	42.5	42.2
DMI	31.6	24	7.1	20	30.1	38.1	38
ICTP	33.3	21.3	6.8	20.4	26.2	35.8	35.3
KNMI	33.8	22.3	6.8	20.6	27.8	36.5	36.3
MPI	34.1	21.1	6.3	20	25.5	36.3	34
SMHCI	34.6	21	5.9	18.7	25.7	36.7	34.3
mean	**33.24**	**23.21**	**7.04**	**20.11**	**28.75**	**38.27**	**37.38**
spread	**1.02**	**2.46**	**0.96**	**0.72**	**3.04**	**2.81**	**3.36**

3.3. Conrad index

The mean Conrad index value is smaller than the Gorczynsky one in South, South-East, and East-Europe, respectively, according to each model (*Table 6*). The difference between the two indexes is the largest in Great-Britain due to the denominator and the smallest in East-Europe in the 2021–2050 period. In the 2071–2100 period, larger continental influence is predicted by the Conrad index than by the Gorczynsky in Scandinavia area, while the difference between the two index is the smallest in Central Europe according to ARPÈGE driven and in East-Europe according to ECHAM5 driven RCMs, respectively. The predicted change of the Gorczynsky index is larger than the predicted change of the Conrad index in almost each region in both time periods (*Fig. 5*).

The distinction among the different GCM driven model results is analogous with the differences in the case of the temperature anomaly. The change of the Conrad index value in time is the same than in the case of the Gorczynsky index. Similarly to the Gorczynsky index, the largest Conrad index values are predicted by CNRM in Central, South-East and East Europe, respectively, in 2071–2100. The change of the modeled and measured difference values in time and the spread of the model results (*Table 7*) are also analogous with the Gorczynsky index ones.

Table 6. Space differences of the predicted mean Conrad index C_{mean} in 2021–2050 (top) and 2071–2100 (bottom) for the regions defined in *Table 2*

	Conrad index in 2021–2050						
Region	**ARPÈGE** C_{mean}	**CNRM** C_{mean}	**DMI** C_{mean}	**ICTP** C_{mean}	**KNMI** C_{mean}	**MPI** C_{mean}	**SMHCI** C_{mean}
1	27.2	27.2	26.1	27.7	27.8	27.8	28.4
2	22.7	23.0	22.1	21.9	22.0	22.0	21.6
3	10.7	11.0	10.2	10.6	10.6	10.3	10.0
4	**26.3**	26.7	26.4	27.1	27.1	26.3	26.3
5	29.4	29.1	28.9	28.0	28.1	27.8	27.3
6	34.9	34.6	32.3	32.1	32.1	32.0	31.9
7	38.4	38.1	36.7	35.0	35.4	34.7	34.4
	Conrad index in 2071–2100						
Region	**ARPÈGE** C_{mean}	**CNRM** C_{mean}	**DMI** C_{mean}	**ICTP** C_{mean}	**KNMI** C_{mean}	**MPI** C_{mean}	**SMHCI** C_{mean}
1	30.7	30.8	29.8	31.3	31.7	32.0	32.3
2	26.2	27.9	24.9	22.5	23.5	22.4	22.3
3	11.0	12.3	10.7	10.4	10.5	9.9	9.6
4	23.8	24.6	23.7	24.0	24.2	23.7	22.4
5	31.9	34.5	30.6	27.2	28.6	26.5	26.7
6	39.1	39.5	35.7	33.7	34.4	34.2	34.5
7	40.6	41.1	37.4	35.0	35.9	33.8	34.14

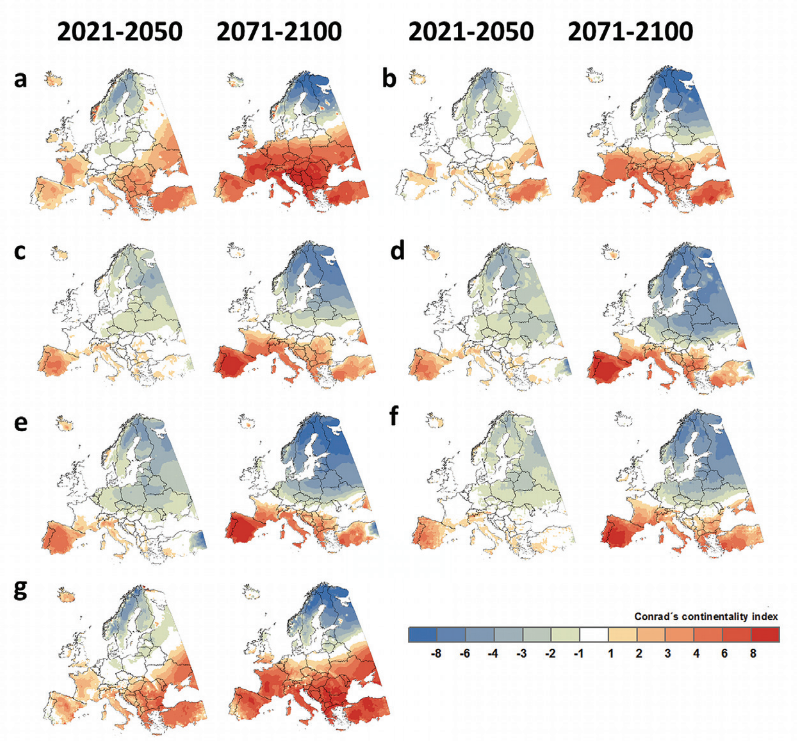

Fig. 5. Predicted changes of the Conrad indexes (a) CNRM, (b) DMI, (c) KNMI, (d) MPI, (e) SMHIRCA, (f) ICTP, and (g) ARPÈGE.

3.4. Central Europe

The continentality in Central Europe is detailed by the ALADIN-Climate/CZ (hereinafter referred to as CHMI) model with higher (10 km) horizontal resolution. The model has same dynamical core as CNRM, but they differ significantly in their physical package (*Skalak et al.,* 2008). Its physical package is detailed in *Farda et al.* (2010). CHMI is run in CECILIA domain which focuses on the Czech Republic and its vicinity. The results of simulated and observed Gorczynsky and Conrad indexes are presented in *Figs. 6* and *7*, respectively. *Table 8* shows the mean value and predicted change value of temperature amplitude, Gorczynsky index, and Conrad index, respectively in the 2021–2050 and 2071–2100 periods.

Table 7. The spread of the simulated Conrad index of the models in 2021–2050 (top) and in 2071–2100 (bottom) for the regions defined in *Table 2*

Spread of simulated Conrad index 2025–2050							
	1	**2**	**3**	**4**	**5**	**6**	**7**
ARPÈGE	27.2	22.7	10.7	26.3	29.4	34.9	38.4
CNRM	27.2	23	11	26.7	29.1	34.6	38.1
DMI	26.1	22.1	10.2	26.4	28.9	32.3	36.7
ICTP	27.7	21.9	10.6	27.1	28	32.1	35
KNMI	27.8	22	10.6	27.1	28.1	32.1	35.4
MPI	27.8	22	10.3	26.3	27.8	32	34.7
SMHCI	28.4	21.6	10	26.3	27.3	31.9	34.4
mean	**27.45**	**22.18**	**10.48**	**26.6**	**28.37**	**32.84**	**36.1**
spread	**0.72**	**0.48**	**0.33**	**0.36**	**0.76**	**1.31**	**1.64**
Spread of simulated Conrad index 2070–2100							
	1	**2**	**3**	**4**	**5**	**6**	**7**
ARPÈGE	30.7	26.2	11	23.8	31.9	39.1	40.6
CNRM	30.8	27.9	12.3	24.6	34.5	39.5	41.1
DMI	29.8	24.9	10.7	23.7	30.6	35.7	37.4
ICTP	31.3	22.5	10.4	24	27.2	33.7	35
KNMI	31.7	23.5	10.5	24.2	28.6	34.4	35.9
MPI	32	22.4	9.9	23.7	26.5	34.2	33.8
SMHCI	32.3	22.3	9.6	22.4	26.7	34.5	34.14
mean	**31.22**	**24.24**	**10.62**	**23.77**	**29.42**	**35.87**	**36.84**
spread	**0.86**	**2.17**	**0.87**	**0.68**	**3.02**	**2.42**	**2.98**

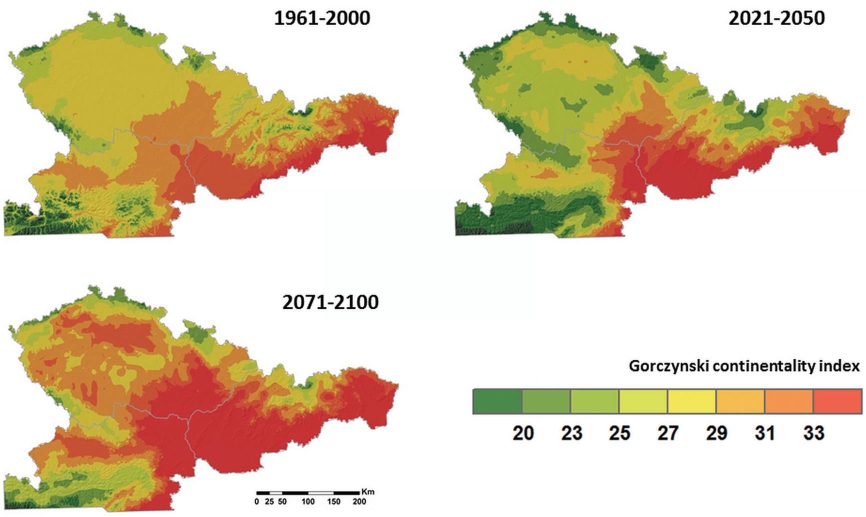

Fig. 6. ALADIN/CZ simulated and higher resolution observed Gorczynsky index in CECILIA domain.

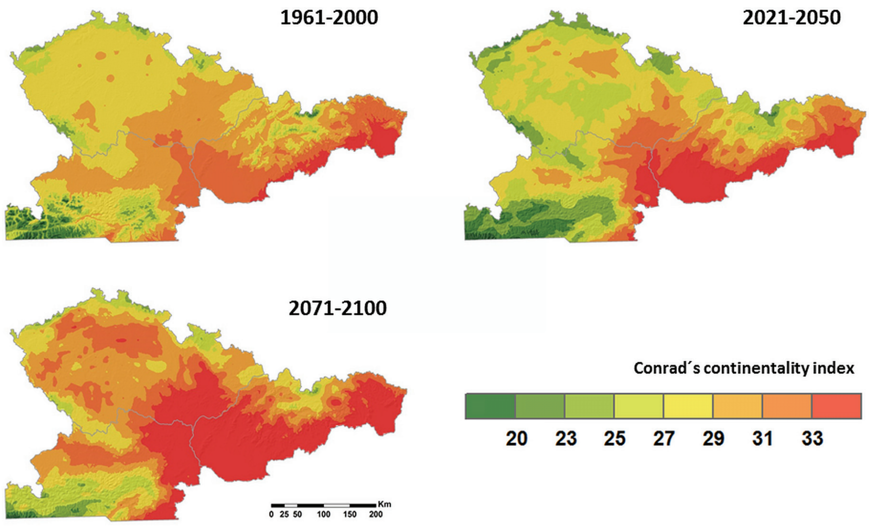

Fig. 7. ALADIN/CZ simulated and higher resolution observed Conrad index in CECILIA domain.

Table 8. The mean value and predicted changes of annual temperature amplitude, Gorczynsky and Conrad continentality indexes, respectively, predicted by the ALADIN-Climate/CZ model for the near and far future time slices, respectively

	ALADIN-CLIMATE/CZ			
	2021–2050		2071–2100	
	T_{MEAN}	$T_M–T_E$	T_{MEAN}	$T_M–T_E$
Temperature amplitude	21.3	–0.3	22.8	1.2
Gorczynsky index	27.6	–0.7	31.1	2.7
Conrad index	28.3	–0.6	31.4	2.4

Comparing the CHMI and ENSEMBLES model results, the differences are the smallest between CHMI and ICTP or KNMI values in 2021–2050, while in the further period the distinction is the smallest between the ARPÈGE and CHMI predicted continentality indexes. The predicted change value is negative in the near and positive in the far future, respectively, like in the DMI case. Based on the mean Gorczynsky index, the climate will be transitional maritime according to CHMI in Central Europe, which agrees with the other ENSEMBLES model results with the exception of the CNRM prediction to the 2071–2100 time slice.

The differences between the CNRM and CHMI predicted mean continentality values is 0.8 in the case of both indexes in the near future time slice, while the differences between the Gorczynsky and Conrad indexes are 3.4 and 3.1, respectively, in the far future period. Some factors which could be responsible for these differences are the large/small integrated area, higher/lower resolution, and the differences between the models. CHMI results positive precipitation bias due to high accumulation of snow in Central Europe during late winter and early spring in both of the 50 km and 10 km resolution cases (*Farda et al.,* 2007; *Skalak et al.,* 2008). This wetter feature of precipitation field corresponds well to the negative bias in winter and spring mean temperature. Furthermore, *Farda et al.* (2007) found that the smaller domain size enhances the precipitation due to the unrealistic generation of vertical velocity in the coupling zone of the model which affects directly even the interior of the rather limited domain.

4. Discussion

4.1. Effect of drivers

We found that the drivers have a significant effect on the spread of results. According to the ECHAM5 driven RCMs, the Atlantic Ocean has a strong influence on the surface temperature due to the too zonal large-scale circulation and underestimated sea-ice condition of the ECHAM5-r3 GCM. Thanks to this phenomenon, smaller continentality indexes were predicted by the ECHAM5 driven RCMs than the ARPÈGE forced ones in each regions except in South-Europe in both time periods.

4.2. Effect of model resolution

The higher resolution model provided finer details of the simulated field, but the resolution differences did not play dominant role in the difference from other RCM results. Small differences were found between the results of ARPÈGE 50 km and CNRM 25 km resolution models. The finer resolution ALADIN-Climate/CZ resulted similar results like ITCP or KNMI in the nearer future, while its results were closer to the ARPÈGE simulation in the far future case. The CHMI simulated mean continentality indexes decreased compared to the observed values in the 2021–2050 time period, while increased in the far future slice. The differences between the CNRM and CHMI results probably come from the positive wet bias of CHMI, which is persistent when smaller domain is used.

4.3. *Impacts on continentality*

Two different continentality indexes (Gorczynsky and Conrad, respectively) were calculated in function of annual temperature anomaly and sinus function of latitude. The mean annual temperature range rises with increasing distance from the ocean and with increasing aridity. Both continentality indexes strongly depend on the annual temperature range, and their spatial differences are well correlated with the space differences of temperature anomaly. The largest continental effect in South-Europe came from the block of maritime airmass caused by the Pyrenees. The continentality indexes decreased with time only in Scandinavia region. This phenomenon can be explained with the assumption of the melting of sea-ice which causes larger SST. Despite the fact that the maximum internal variability of RCMs is in the South-East European region (*Sanchez-Gomez, E. et al.,* 2009), the largest model variability was in the Scandinavia region in each model case. This maximum variability affected by the natural variability is caused by SST and sea-ice condition.

5. *Conclusion*

The future continental climate is simulated by applying two different continentality indexes: the Gorczynsky and Conrad, respectively. Both of them indicate the continentality as a function of the annual mean temperature anomaly and a sinus function of the latitude angle. The largest difference between their index values is caused by the boundary condition which is applied in the Conrad approach to avoid the insensible negative continentality values in lower latitudes. In our simulation, the isoline flows near meridionally only in East-Europe, and it flows to eastward direction in South-East and South Europe, respectively. The greatest change with time slice in isoline direction is in Scandinavia, where the climate becomes more balanced maritime despite the resulted larger model variability.

The core message of our research is whether Central Europe becomes more continental or maritime according to the A1B RCM scenarios in the 21st century?

The climate of Central Europe is predicted to be transitional maritime according to the mean Gorczynsky index of RCMs with exception of CNRM in the further time slice. This result might be explained by the experience that CNRM overestimates the monthly maximum temperature and underestimates the precipitation in Central Europe. The simulated continental influence will diminish compared to the observed state according to the ECHAM5 driven RCMs in Central Europe in both time slices. Although the boundary of maritime and continental climate run along east Austria, south-east Czech Republic, and mid-Slovakia according to the CHMI detailed Gorczynsky index, its mean value is below the continental boundary.

Acknowledgements: This research was supported by the Czech Grant Agency in the frame of the project: Global and regional climate model simulations in Central Europe in the 18th-20th centuries in comparison with observed and reconstructed climate, GACR P209/11/0956. Pavel Zahradníček was supported by project InterSucho (no. CZ.1.07/2.3.00/20.0248). We are thankful for the E-OBS data set from the EU-FP6 project ENSEMBLES (http://www.ensembles-eu.org) and the data provided by the ECA&D project (http://www.eca.knmi.nl). Data for Central Europe was performed within the CECILIA project, funded by the European Commission's 6th Framework Programme under contract number 037013.
We also would like to thank to the anonymous reviewers for their comments and suggestions.

References

Conrad, V. and *Pollak, L.W.,* 1950: Methods in climatology. 2nd edition. Harvard university press, Cambridge, Massachusetts.

Christensen, J.H., *Christensen, O.B., Lopez, P., Van Meijgaard, E.,* and *Botzet*, *M.,* 1996: The HIRHAM4 regional atmospheric model. Scientific Report 96-4, The Danish Meteorological Institute, Copenhagen, Denmark.

Christensen, J.H., *Boberg, F., Christensen, O.B.,* and *Lucas-Picher*, *P.,* 2008: On the need for bias correction of regional climate change projections of temperature and precipitation. *Geophys. Res. Lett. 35*, L20709.

Currey, D.R., 1974: Continentality of Extratropical Climates. *Ann. Ass. Amer. Geograph. 64,* 268–280.

Déqué, M., Rowell, D. P., Lüthi, D., Giorgi, F., Christensen, J.H., Rockel, B., Jacob, D., Kjellström, E., de Castro M., and *van den Hurk, B.,* 2007: An intercomparison of regional climate simulations for Europe: assessing uncertainties in model projections. *Climate Change* 81 (Suppl. 1), 53–70.

Déqué, M., *Somot, S., Sanchez-Gomez, E., Goodess, C.M., Jacob, D., Lenderink G.,* and *Christensen, O.B*., 2012: The spread amongst ENSEMBLES regional scenarios: regiona climate models, driving general circulation models and interannual variability. *Clim. Dynam*. *38*, 951–964.

Dirscoll, D.M. and *Yee Fong, J.M.,* 1992: Continentality: A basic climatic parameter re-examined. *Int. J. Climat. 12*, 185–192.

Dosio, A. and *Paruolo, P.*, 2011: Bias correction of ENSEMBLES high-resolution climate change projections for use by impact models: Evaluation on the present climate. *J. Geophys. Res*. *116*, D16106.

Farda, A. Štěpánek, P., Halenka, T., Skalák, P., and *Beld*, *M.,* 2007: Model ALADIN in climate mode forced with ERA40 reanalysis (course resolution experiment). *Meterologický časopis 10*, 123–130.

Farda, A., M. Dequé, S. Somot, A. Horányi, V. Spiridonov and *H. Tóth*, 2010: Model ALADIN as regional climate model for central and eastern Europe*. Stud. Geophys. Geod*. *54*, 313–332.

Gibelin, A.-L., and *Déqué, M.*, 2003: Anthropogenic climate change over the Mediterranean region simulated by a global variable resolution model. *Clim. Dynam*. *20*, 327–339.

Giorgi, F. Bi, X., and *Pal*, *J.S.,* 2004: Mean, interannual variability and trends in regional climate change experiment over Europe. I. Present-day climate (1961-1990). *Clim. Dyn*am. *22*, 733–756.

Gorczynsky, L., 1922: The calculation of the degree of continentality. *Mon. Weather Rev. 50*, 370.

Hasselmann, K., 1976: Stochastic climate models. Part I: Theory. *Tellus 28*, 473–485.

Haylock M.R., Hofstra, N., Klein Tank, A.M.G., Klok, E.J., Jones P.D., and *New*, *M.,* 2008: A European daily high-resolution gridded data set of surface temperature and precipitation for 1950–2006, *J. Geophys*. *Res*. *113*, D20119.

Hewitt, C.D. and *Griggs, D.J.*, 2004: Ensembles-based predictions of climate changes and their impacts. *Eos Trans. AGU* 85, 566.

Hofstra, N., *M. New, C. McSweeney*, 2010: The infulence of interpolation and station network density on the distributions and trends of climate variables in gridded daily data. *Climate Dynam. 35*, 841–858.

Holmlund, P. and *Schneider, T.*, 1997: The effect of continentality on glacier response and mass balance. *Ann. Glaciology 24*, 272–276.

Jacob, D., 2001: A note to the simulation of the annual and inter-annual variability of the water budget over Baltic Sea drainage basin. *Meteorol. Atmos. Phys. 77*, 61–73.

Johansson, O.V., 1926: Uber die asymmetrie der meteorologischen Schwankungen. In.: Soc. Sci. Fennica, Commentationes Phys. Math., 3, 1ff

Kjellström, E., *L. Bärring, S. Gollvik, U. Hansson, C. Jones, P. Samuelsson, M. Rummukainen, A. Ullerstig, U. Willén* and *K. Wys,* 2005: A 140-year simulation of European climate with the new version of Rossby Central regional atmospheric climate model (RCA3). *SMHI Reports Meteorology and Climatology 108*, SMHI, SE-60176. Norrköping, Sweden.

Kjellström, E., *G. Nikulin, U. Hansson, G. Strandberg* and *A. Ullersting*, 2011: 21st century changes in the European climate: uncertainties derived from an ensemble of regional climate model simulations. *Tellus 63A*, 24–40.

Klein Tank, A.M.G., *J. B. Wijngaard1, G. P. Können, R. Böhm, G. Demarée, A. Gocheva, M.Mileta, S. Pashiardis, L. Hejkrlik, C. Kern-Hansen, R. Heino, P. Bessemoulin, G. Müller-Westermeier, M. Tzanakou, S. Szalai, T. Pálsdóttir, D. Fitzgerald, S. Rubin, M. Capaldo, M. Maugeri, A. Leitass, A.Bukantis, R. Aberfeld, A. F. V. van Engelen, E. Forland, M. Mietus, F. Coelho, C. Mares, V.Razuvaev, E. Nieplova, T. Cegnar, J. Antonio López, B. Dahlström, A. Moberg, W. Kirchhofer, A. Ceylan, O. Pachaliuk, L. V. Alexander and P. Petrovic*ˇ 2002: Daily dataset of 20th century surface air temperature and precipitation series for the European climate asseessment. *Int. J. Climatol. 22*, 1441–1453.

Lenderink, G., *B. van den Hurk, E. van Meijgaard, A. van Ulden* and *H. Cuijpers*, 2003: Simulation of present-day climate in RACMO2: first results and model developments. *Technical Report TR-252*, Royal Netherlands Meteorological Institute.

van der Linden, P. and *Mitchell, J.F.B.* (eds.) 2009: ENSEMBLES: Climate Change and its Impacts: Summary of research and results from the ENSEMBLES project. Met Office Hadley Centre, FitzRoy Road, Exeter EX1 3PB, UK.

McBoyle, G.R., and *Steiner, D.,* 1972: A factor-analytic approach to the problem of continentally. *Geografiska Annaler Series* A, *Physical Geography, 54*, 12–27.

Meier, H.E.M., *Höglund, A., Döscher, R., Andersson, H., Löptien, U.,* and *Kjellström, E.,*2011: Quality assessment of atmospheric surface fields over the Baltic Sea from an ensemble of regional climate model simulations with respect to ocean dynamics. *Oceanologia 53*, 193–227.

Mikolaskova, K., 2009: A regression evaluation of thermal continentality. *Geografie 4*, 350–361.

Nakicenovic, N. and *Swart*, *R.,* 2000: Special Report on Emissions Scenarios: A Special Report of Working Group III of the Intergovernmental Panel on Climate Change, Cambridge UK: Cambridge University Press.

Nikiforova, T., *Savytskyi, M., Limam, K., Bosschaerts, W.,* and *Belarbi*, *R.,* 2013: Methods and results of experimental researches of thermal conductivity of soils. *Energy Procedia 42*, 775 – 783.

Placová, E. and *Kyselý, J.,* 2010: Evaluation of daily temperatures in Central Europe and their links to large-scale circulation in an ensemble of regional climate models. *Tellus 63A*, 763–781.

Rowell, D.P. and *Zwiers, F.W.,* 1999: The global distribution of sources of atmospheric decadal variability and mechanisms over the tropical Pacific and southern North America. *Clim. Dynam. 15*, 751–772.

Sanchez-Gomez, E., *Somot, S.,* and *Déqué*, *M.,* 2009: Ability of an ensemble of regional climate models to reproduce weather regimes over Europe-Atlantic during the period 1961-2000. *Clim. Dynam*. *33*, 723–736.

Skalak, P., *Štěpánek, P.,* and *Farda, A.,* 2008: Validation of ALADIN-Climate/CZ for present climate (1961-1990) over the Czech Republic. *Idojaras 112*, 191–201.

Sládek, I., 2005: Návrh nové míry kontinentality klimatu. *Fyzickogeografický sborník*, *3*,. 144–147. (In Slovak)

Solomon, S., *Qin, D., Manning, M.,* 2007: Technical Summary. In: (Eds.: *S. Solomon, D. Qin, M. Manning, Z. Chen, M. Marquis, K. B. Averyt, M. Tignor* and *H. L. Miller*.) Climate Change 2007: The Physical Science Basis. Contribution of Working Group I to the Fourth Assessment Report of the Intergovernmental Panel on Climate Change. Cambridge University Press, Cambridge, United Kingdom and New York, NY, USA.

Štěpánek, P., *Zahradníček, P., Brázdil, R.,* and *Tolasz*, *R.*. 2011a: Metodologie kontroly a homogenizace časových řad v klimatologii Český hydrometeorologický ústav: Praha. (in Czech).

Štěpánek, P., *Zahradníček, P.,* and *Huth*, *R.,* 2011b: Interpolation techniques used for data quality control and calculation of technical series: an example of a Central European daily time series. *Időjárás 115*, 87–98.

Štěpánek, P., *Zahradníček, P.,* and *Farda*, *A.,* 2013: Experiences with data quality control and homogenization of daily records of various meteorological elements in the Czech Republic in the period 1961–2010. *Időjárás 117*, 123–141.

Wilby R.L., *Wigley, T.M.L., Conway, D., Jones, P.D., Hewitson, B.C., Main, J.,* and *Wilks*, *D.S.,* 1998: Statistical downscaling of general circulation model output, a comparison of Methods. *Water Resour. Res*. *34*, 2995–3008.